The K/HDEL receptor does not recycle, but instead acts as a Golgi-gatekeeper

Jonas Alvim
University of Leeds
Robert Bolt
University of Leeds
Jing An
University of Leeds
Yasuko Kamisugi
University of Leeds https://orcid.org/0000-0002-5265-3658
Andrew Cuming
University of Leeds https://orcid.org/0000-0003-2562-2052
Fernanda Silva-Alvim
University of Leeds
Meiyi Hu
University of Leeds
Dominique Hirsz
University of Leeds
Jurgen Denecke (j.denecke@leeds.ac.uk)
University of Leeds

Article

Keywords:

Posted Date: July 14th, 2022

DOI: https://doi.org/10.21203/rs.3.rs-1781070/v1

Version of Record: A version of this preprint was published at Nature Communications on March 23rd, 2023. See the published version at https://doi.org/10.1038/s41467-023-37056-0.

Abstract

The K/HDEL receptor (ER retention defective 2 or ERD2) does not recycle between compartments when sorting ER chaperones, contrary to the favoured model. A conserved C-terminal di-leucine motif specifically prevents ERD2 Golgi-to-ER transport and is not required for ER export. The Golgi-retention mechanism strips Golgi-membranes of the GTPase ARF1 so that ERD2 avoids accompanying its ligands in retrograde transport. When this motif is deleted or masked, introducing a fast ER-to-Golgi export signal or an alternative *cis*-Golgi retention signal re-activates ERD2. Meanwhile, forcing retrograde transport renders the receptor non-functional. We have established an in vivo ligand/receptor ratio far greater than 100 to 1, and propose a gatekeeper model to explain how few receptors at the Golgi can prevent the secretion of highly abundant soluble ER proteins. The underlying mechanism is conserved across kingdoms and will yield valuable insight into Golgi-mediated cargo sorting and cisternal compartment maintenance.

Introduction

The Golgi apparatus plays a central role in sending and receiving membrane carriers to and from organelles of the secretory pathway. Its evolutionary origin is unknown, and how it maintains its identity despite the constant influx and efflux of transport vesicles continues to fascinate and divide the field[1,2,3]. Membrane-spanning sorting receptors are a particularly interesting class of proteins as they mediate the sorting of cargo but need to be sorted themselves.

A central dogma to describe receptor-mediated transport was derived from the principle of receptor-mediated endocytosis at the plasma membrane[4]. A prominent example is the mannose-6-phosphate (M6P) receptor which binds lysosomal proteins in the Golgi, moves in clathrin coated vesicles to early endosomes, followed by ligand-release and receptor recycling back to the Golgi[5,6]. Continuous recycling[7] permits few receptors to sort many lysosomal proteins, and this was shown to be essential for vacuolar sorting in yeasts[8] and plants[9]. Well-defined receptor mutants with defects in either anterograde or retrograde transport strongly support the recycling model[10,11].

Evidence that a similar recycling principle operates for highly abundant soluble ER residents bearing the KDEL or HDEL retention signal first arose from the detection of post-translational modifications that are Golgi-specific[12,13]. An elegant genetic screen led to the identification of the K/HDEL receptor (ERD2) in yeast[14], followed by the isolation of the human homologue[15]. Ligand-overproduction caused human ERD2 redistribution from the Golgi to the ER[16], and the receptor-recycling principle was generally accepted by the field. Since detection of endogenous ERD2 proved technically difficult[17,18], the field used C-terminal ERD2 fusions for subcellular localisation and the demonstration of ligand-induced ERD2 redistribution to monitor its activity indirectly[16,19–22].

Having recently shown that fluorescent proteins such as YFP or RFP fused to the ERD2 C-terminus inactivate the receptor, we constructed a new fluorescent fusion (YFP-TM-ERD2) in which the ERD2 core

remains unobstructed[23]. This fusion was only detected at the Golgi apparatus even when ligands were overproduced. Both the Golgi residency and biological activity of ERD2 were found to be strictly dependent on a native C-terminus harbouring a novel di-leucine motif (LXLPA)[23]. We concluded that this signal either mediates extremely fast “frequent flyer” ER export of ERD2 to explain the steady state levels at the Golgi, or that ERD2 may not recycle as currently believed.

Here, we provide a systematic set of experiments that strongly reject a “frequent flyer” model, and show that a Golgi-retention mechanism averts retrograde receptor transport to the ER. We discuss the implications for understanding Golgi-identity and how sorting machinery segregates from cargo.

Results

YFP-TM-ERD2 can replace endogenous ERD2 in *Nicotiana benthamiana* and *Physcomitrium patens*

To obtain genetic validation for the new fluorescent fusion[23], we tried to generate stable *Nicotiana benthamiana* transformants co-expressing an ERD2ab antisense construct in a T-DNA together with either YFP-TM-ERD2 or ST-YFP-HDEL as control (Figure 1A). The frequency of control callus-formation was very low; shoots revealed the typical ER network for ST-YFP-HDEL (Figure 1B, panel 1) but failed to form roots. All control lines were subsequently lost, confirming that ERD2 knockdown is lethal[24]. In sharp contrast, co-expressed YFP-TM-ERD2 resulted in fertile plants, showing punctate Golgi-structures (Figure 1B, panel 2). Seeds also produced fertile plants, and root cortex cells displayed typical Golgi structures (Figure 1B, panel 3). YFP-TM-ERD2 did not reveal any detectable ER network, even at the highest detector gain and contrast.

Further validation was also provided in the model bryophyte *Physcomitrium patens* using targeted “knock-in” of YFP-TM, followed by complete deletion of the second ERD2 gene (Figures 1C,D). The resulting moss-line showed normal growth expressing YFP-TM-ERD2 in punctate structures in the growing tips and newly formed cell plates (Figure 1E, panel 1, white stars). Expression was very low and high detector gain settings were needed, therefore also revealing autofluorescence of chloroplasts (Chl.). No structures reminiscent of ER were observed (Figure 1E, panel 2, white arrow heads). The results establish that a single YFP-TM-ERD2 gene expressed under its native promoter can functionally replace both endogenous ERD2 genes in *P. patens*.

Golgi residency of ERD2 is strictly linked to functionality in eukaryotes

To rule out that ERD2 Golgi residency is a plant-specific feature, ERD2 orthologs from 12 further eukaryotic organisms were tested in our functional assay[23]. Figure 2A shows that the vast majority of ERD2 orthologs increased Amy-HDEL or Amy-KDEL retention in the cells comparable to *Arabidopsis thaliana* ERD2 (AtERD2 - second lane). Below a threshold of 50% homology with AtERD2, Amy-HDEL secretion was only weakly reduced (*T. brucei*) or not reduced at all (*K. lactis, S. cerevisiae*). *S. cerevisiae*

ERD2 (ScERD2 – last lane) consistently induced AmyHDEL secretion, suggesting a dominant-negative effect on endogenous machinery.

Human ERD2 (HsERD2) mediates a very similar ER retention activity as AtERD2, as illustrated by a dose-response assay (Supplemental figure 3A), and shares the same sensitivity to C-terminal fusions as plant ERD2[23]. YFP-TM-HsERD2 was found exclusively in the Golgi whilst the C-terminal fusion displayed a dual ER-Golgi localisation (Figure 2B). The former promoted strong Amy-HDEL retention whilst the latter did not (Figure 2C).

An earlier study of the human ERD2 C-terminus proposed that Serine209 controls ARF-GAP recruitment via PKA phosphorylation[21]. In our activity assay, neither the inactive (S209A) nor the phosphomimetic (S209D) mutation affected ERD2 function and the residue is not conserved between plant and human ERD2 (Figure 2D). More recently, a “cluster of lysines” near the ERD2 C-terminus was proposed to form an inducible COPI-retrieval motif[22]. Here we show that mutating each lysine (K206, K207) or both together does not alter the biological activity of human ERD2 (Figure 2C, Supplemental figure 3B). Instead, the conserved leucines at position -3 and -5 from the C-terminus (Figure 2D) are essential for human ERD2 activity (Figure 2C, last lane). A strict Golgi-localisation of human ERD2 mutants with wild type amy-HDEL retention activity was observed (Figure 2E) whilst additional labelling of the ER network was only seen when the leucines were mutated (LLGG).

To test if the ERD2-C-terminus can tolerate small epitopes as for instance the c-myc epitope[16], we tested 3 different tags on either plant or human ERD2 for activity and localisation (Figure 2F). FLAG- and c-myc-tagged ERD2 showed strongly reduced biological activity compared to untagged ERD2 (Figure 2G) and were localised to both the ER and the Golgi (Figure 2H). A dose-response assay illustrates how strongly those two tags affected the functionality of plant and human ERD2 (Supplemental figure 3C) although weak residual activity may suffice for yeast complementation[14]. Interestingly, fusion of the HA tag (YPYDVPDYA) had only a minor effect on either plant or human ERD2 activity and resulted in predominant Golgi localisation (Figure 2H). This exception highlights the temperamental nature of C-terminal modifications, but also shows the strict correlation between Golgi residency and strong biological activity.

The C-terminal di-leucine motif of ERD2 prevents its recycling to the ER

To test if the di-leucine motif is a fast ER to Golgi export signal, fluorescence recovery after photobleaching (FRAP) was used to see if YFP-TM-ERD2 arrival at the Golgi is slowed down by mutating the signal. Figure 3A shows that the opposite is observed; the mutant recovers approximately twice as fast. Compared to the Golgi marker ST-YFP, the wild type ERD2 fusion behaves very similar and does not exhibit unusually fast “frequent-flyer” ER export to start with (Supplemental figures 4A, B). The results show that the di-leucine motif acts as a Golgi-retention signal, it prevents Golgi to ER retrograde transport

rather than accelerating ER export. A faster Golgi-recovery of the mutant can be explained by the additional pool of ERD2 in the ER (Supplemental figure 4C) which supplements de novo synthesized ERD2 for more ER export.

To show that Ligand-induced ERD2 redistribution to the ER[20,22,25] could be caused by compromised Golgi-retention, we co-expressed secreted Amy or retained AmyHDEL together with either functional or non-functional ERD2-fusions (Figure 3B). YFP-TM-ERD2 shows no HDEL-mediated redistribution (Figure 3C). Deletion of the last 5 amino acids LQLPA (YFP-TM-ERD2ΔC5) results in partial ER localisation which is exacerbated upon HDEL-overdose (Figure 3D). The same HDEL ligand-induced redistribution from Golgi to ER can be seen with ERD2-YFP (Figure 3E). Interestingly, low expression of ERD2-YFP alone also favours an ER-localisation (Figure 3F, Supplemental Figure 5A). ERD2-YFP failed to yield rooted transgenic plants when co-expressed with ERD2ab antisense construct and weak ERD2-YFP fluorescence was mainly detected in the ER (Supplemental Figure 5B panels b3, b4). As the ERD2ab antisense was expressed from the same T-DNA, high expressing lines did not even reach the shoot stage.

The results show that ligand-mediated ER redistribution of ERD2 is simply caused by masking the di-leucine motif. Interestingly, ERD2 leakage to post-Golgi organelles remains undetectable in all conditions, suggesting that an additional mechanism prevents post-Golgi transport.

The Golgi-retention motif is required to inhibit COPI-mediated recycling.

It has been reported that ERD2 can cause mixing of Golgi and ER membranes[26] by recruiting ARF1-GAP to the Golgi apparatus[27]. We therefore tested the influence of wild type and mutant ERD2 on the localisation of the GTPase ARF1. ARF1 typically colocalises with the Golgi-marker ST-RFP and post-Golgi structures (Figure 4A, white arrowheads), but when co-expressed with ERD2, ST-RFP redistributes to an ER-like super-compartment reminiscent of Brefeldin A treatment[19] and ARF1 redistributes to the cytosol. ERD2 inhibits Amy-HDEL secretion at low expression levels without affecting constitutive Amy secretion[23] but at saturating expression levels Amy secretion is also inhibited (Figure 4B). The deletion mutant ERD2ΔC5 affects neither Amy-HDEL retention nor Amy secretion. The results strongly suggest that ERD2 inhibits COPI-mediated transport, and that the Golgi-retention motif is required for this. Although ERD2 has been reported to interact with ARF1 this was based on inactive C-terminal fusions[25].

COPII/COPI-mediated recycling of ERD2 is incompatible with its biological function

To test COPI-dependence more directly, we created an ERD2 hybrid (Figure 4C) by replacing the 9 most C-terminal amino acids with those of a P24 family member (p24δ5, AT1G21900), harbouring the di-hydrophobic sequence (YF) for COPII-mediated ER export and a canonical di-lysine motif (KKXX) for COPI-mediated recycling[28,29].

The hybrid showed no biological activity on HDEL cargo, but mutating the two lysines into serines (KKSS) induced receptor activity again (Figure 4D). CLSM analysis revealed complete ER retention of RFP-TM-ERD2::P24tail, with no detection in the Golgi bodies (Figure 4E, white arrow heads), illustrating the dominant nature of the COPI sorting signal. Destroying the COPI signal by replacing the two lysines with serines establishes predominant Golgi-residency with only traces detectable in the ER (Figure 4E).

Canonical COPI transport is clearly incompatible with ERD2 function, but the proposed COPII ER export signal in the p24 C-terminus[29] seems to compensate for the lack of the di-leucine Golgi retention signal.

An alternative Golgi-retention signal can re-activate ERD2-YFP

To test if the di-leucine motif can be replaced by an alternative Golgi localisation signal, of ERD2, we chose the newly identified N-terminal cytosolic Golgi retention motif (LPYS) of Arabidopsis thaliana α-mannosidase I (MNS3) that mediates cis-Golgi localisation[30]. We first show that YFP-TM-ERD2 colocalises better with MNS3-RFP than with ST-RFP (Figure 6A,B). We supplemented inactive ERD2-YFP with the same N-terminal TM domain as in previous constructs (TM-ERD2-YFP) and then introduced the MNS3 N-terminus harbouring the LPYS signal (LPYS-TM-ERD2-YFP). The Amy-HDEL cargo sorting assay (Figure 6C) confirms that TM-ERD2 has almost wild type activity[23]. TM-ERD2-YFP has lost this activity due to the devastating effect of C-terminally fused YFP. However, LPYS-TM-ERD2-YFP was partially re-activated despite the masked C-terminus. TM-ERD2-YFP remains partially ER-localised whilst LPYS-TM-ERD2-YFP is exclusively detected in the Golgi bodies (Figure 6D).

The results provide strong evidence that Golgi-retention per-se promotes ERD2 function, directly arguing against the receptor recycling model.

ERD2 mediates extra-stoichiometric retention of HDEL proteins

To establish relative numbers of ectopically expressed ERD2 versus Amy-HDEL proteins in vivo, we used quantitative immunoprecipitation with excess antibodies after 8 hours of continuous metabolic ^{35}S labelling. HA-tagged ERD2 had the highest biological activity of all tagged ERD2 variants (Figure 2G), therefore we expressed this receptor and Amy-HDEL from two separate GUS reference vectors to ensure comparable transfection efficiencies.

Despite equalised plasmid transfection, ERD2-HA produces a weak signal which is dwarfed by the high levels of cellular and secreted Amy-HDEL (Figure 6A). Nevertheless, ERD2-HA co-expression reduced secreted Amy-HDEL levels, accompanied by an increase in the cells. Since exactly two thirds of either cysteine or methionine are found in ERD2 when compared to Amy-HDEL (Figure 6B), the relative number of molecules could be determined by phosphor imaging and multiplying ERD2 values by a factor 1.5.

This shows that there are approximately 4.5 additional Amy-HDEL molecules recovered in the cells for each ERD2 molecule introduced (Figure 6C).

A dose-response experiment with the longer standard 24 hours incubation was carried out using the same transfection conditions for Amy-HDEL and ERD2-HA as in Figure 6A to establish a baseline (Figure 6D, first two lanes). ERD2 plasmid was then progressively diluted up to 100-fold (Figure 6D, all further lanes) whilst the Amy-HDEL plasmid concentration was kept constant. Maximal Amy-HDEL retention was sustained up to 20-fold dilution of the ERD2-HA plasmid. 50-fold and 100-fold dilutions showed only a weak reduction in Amy-HDEL retention. We cannot detect in vivo labelled ERD2 under these conditions, but the internal marker GUS illustrates the quantitative nature of the dose-response assay (Supplemental figure 6A,B).

From these data we can ascertain that one introduced ERD2 molecule can prevent the secretion of well over 100 Amy-HDEL proteins. The true extra-stoichiometric retention capacity is likely to be much higher, because plasmid co-transfection is never 100% complete and ERD2-HA is slightly less active than wild type ERD2. Finally, and most importantly, a protein can only be secreted once, but retention requires endless recycling, as discussed below.

Discussion

The recycling principle for protein sorting receptors has been popular in the field because it is thought to explain how few receptors can transport multiple ligands[7,9,31]. However, whilst vacuolar/lysosomal proteins are sorted only once from secreted proteins, ER residents recycle back to the ER[12], the place where they were originally synthesized. Their perpetual escape to the Golgi would cause an endless “Sisyphus” task for ERD2. In addition, newly synthesized ER residents would add to the burden at each cycle. Given the high abundance of soluble ER residents[32], such odds would defeat even the most efficient receptor, and this conceptual problem has not been widely considered to date. If ERD2 accompanies its ligands to the ER in COPI vesicles, it would need to return to the Golgi as a “frequent-flyer”. Here we have presented a systematic series of results that strongly argue against the frequent flyer recycling principle.

Firstly, lysine residues proposed as an inducible KKXX-like signal for COPI transport[22] were completely irrelevant for ERD2-function (Fig. 2C), and they deviate from the strictly C-terminal position[33]. Secondly, equipping the ERD2 C-terminus with well-established COPII and COPI transport signals[28,29] causes ER localisation and inactivity (Fig. 4), whilst mutating the canonical KKXX motif restores Golgi-localisation and activity.

Two further experiments provide strong arguments for Golgi-retention of ERD2. FRAP analysis shows that the di-leucine motif specifically slows down ERD2 turnover at the Golgi (Fig. 3). The signal is conserved in human ERD2 and promotes both activity (Fig. 2C) and Golgi-residency (Fig. 2E). More importantly, an alternative cis-Golgi retention signal[30] can restore ERD2 function when its di-leucine motif is masked by

YFP (Fig. 6). Finally, ligand-induced redistribution of ERD2 fusions to the ER only occurs when the di-leucine motif is masked or deleted (Fig. 3D,E). This explains previously published data[16,20,22,25] and shows that the discrepancy does not lie with what is observed, but with what is deemed biologically relevant.

It is interesting that masking, mutating or even deleting the di-leucine motif did not lead to ERD2-leakage to post-Golgi compartments. ERD2 may thus contain 2 separate Golgi retention signals, the di-leucine motif to prevent ERD2 retrograde transport and a second to prevent anterograde Golgi-export. The latter remains a mystery[34], as does a full understanding of the mechanisms that maintain the spatial polar organisation of the Golgi stacks themselves[3].

Our measurement of the in vivo ERD2-ligand stoichiometry suggests a ratio higher than 1:100. How can ERD2 avoid the “Sisyphus” paradox? Colloquially, the classic “frequent flyer” model can be illustrated by a taxi-driver who can take only a limited number of passengers. The driver can return to the collection point for another shuttle service, but whilst in transit any additional passengers have to wait. Our results suggest that ERD2 acts more like a “gatekeeper” at the *cis*-Golgi, illustrated by a bouncer who denies entry. Unlike a taxi driver, the bouncer holds its position at the gate and is able to repel a far greater crowd of individuals, including those making repeated attempts. This explains why the Golgi retention motif is crucial for ERD2-function and conserved in eukaryotes (Fig. 2A).

How could ERD2 avoid joining its ligands and maintain its gatekeeper position? We could show that the GTPase ARF1 is stripped from Golgi-membranes and redistributes to the cytosol when ERD2 is overexpressed (Fig. 4A). This is accompanied by inhibition of constitutive secretion (Fig. 4B) and this effect is dependent on the presence of the di-leucine motif for ERD2 Golgi-retention (Fig. 4B). HDEL cargo can be detected in the cis-Golgi[35] and may represent cargo transiently associated with ERD2. ARF1-GAP recruitment[27] may help to retain ERD2 in a COPI-free zone and stimulate/drive ligand-release into an adjacent COPI-coated subdomain.

Permanent Golgi-residency requires only minimal turn-over of ERD2, which explains why its expression under control of its own promoter in P. patens is extremely low (Fig. 1E) and its ER-to-Golgi transport is not faster than that of a typical Golgi marker (Fig. 3A). The gatekeeper model for ERD2 stands apart from the recycling receptors controlling post-Golgi trafficking routes[4,5,6,11] and inspires further thoughts on the unknown origins of the ER and Golgi. When COPI was first associated with retrograde rather than anterograde transport[36,37] the cisternal progression model for Golgi polarity gained momentum[38]. Our present results support the idea that the plant cis-Golgi could be a more permanent core-structure[39] and corresponds to the mammalian ERGIC[40].

A precedent for a sorting facilitator that does not enter the vesicle carrier itself is Tango1, promoting collagen loading for ER export whilst effectively remaining behind in the ER membrane[41,42,43]. Collagen is one of the most abundant secretory cargos in fibroblasts, and a “taxi-driver” mechanism could be easily overwhelmed. An example of a Golgi-resident sorting component is RER1[44], which also depends on its C-

terminus to accumulate in the Golgi apparatus, but it controls accumulation of membrane proteins in the ER. The similarity of ERD2 with sweet transporters[22], which are known to have multiple conformational states[45,46,47], may provide new clues to identify ancient transport mechanisms that could have initiated the formation of an ER-Golgi interface.

Future work should be devoted to experiments exploring 1) how ERD2 maintains its position at the Golgi apparatus without leaking beyond, 2) how it loads K/HDEL cargo for retrograde transport without joining and 3) how anterograde transport of non-ER proteins is achieved whilst the cis-Golgi retains its identity.

Materials And Methods

Recombinant DNA construction

All plasmid constructs were created via standard techniques including PCR amplification, overlap PCR, QuickChange PCR mutagenesis, gene synthesis, oligonucleotide annealing, restriction digests, gel purification and ligation and the E.coli strain for plasmid replication was strain MC1061[48]. Supplementary table 1 lists all plasmids and constructs used from earlier work[23] and new derivatives described below

Double vectors for stable transgenic ERD2 anti-sense lines

For generation of transgenic *N. benthamiana* lines, a nbERD2AB-antisense fragment followed by 3'nos polyadenylation signal was extracted from pJCA60[23] as a NcoI-HindIII, sub-cloned together with a second fragment (BamHI-NcoI, harbouring a 3'ocs polyadenylation signal followed by the CaM35S promoter), into Agrobacterium tumefaciens plant expression vectors pTJA15, pTFLA32 and pTMY1 between BamHI-HindIII. NbERD2AB-antisense mRNA is then transcribed from the strong constitutive CaM35S promoter and the second cassette encodes either ST-YFP-HDEL (pTJCA85), YFP-TM-ERD2b (pTJCA86) or ERD2b-YFP (pTRB29) under the control of weaker TR2 promoter.

Targeted mutagenesis in *P. patens*

Establishment of the YFP-TM-PpERD2B-1/ΔPpERD2B-2 line

For construction of pYFP-TM-ERD2B-1, a fragment containing the YFP-TM sequence from pFLA30[23] was inserted directly between the end of the ERD2B-1 5'-UTR and the start codon of the ERD2B polypeptide coding sequence by overlap PCR, using primers (p1+p2+p3+p4, Supplementary Fig. S1; Supplementary

Table 2). The product, containing 1120bp upstream of the coding region and 803bp genomic DNA commencing from the start codon was cloned into an EcoRV site of pBluescript II KS$^-$. For marker-free knock-in transformation of *P. patens,* 15µg of PCR amplified fragment (primers p5 and p6, Figure 1; Supplementary Fig. S1; Supplementary Table 2) of pYFP-TM-ERD2B-1 containing 1056bp and 760bp of 5' and 3' flanking fragments, respectively, was mixed with 1µg of supercoiled pMBL5 (GenBank Accession No. DQ228130) and used to transform *P. patens* by protoplast-PEG transformation[49]. Primary transformants grown on G418 containing medium were transferred to non-selective medium and initially screened for correct 3'-end targeting by PCR. Loss of the circular selection plasmid was confirmed by sensitivity to G418. The selected transformants were further screened for 5'-end targeting and concatenation events by PCR followed by Southern hybridisation to establish a correctly targeted, single-copy plant. Genomic DNA (2.5µg) was digested with *Hin*dIII for electrophoresis and blotting onto nylon membrane. The probe comprising the 3'-end of YFP and the entire 3'-targeting fragment within *YFP-TM-PpERD2B-1* (Supplementary Fig. S1, shaded box, primers p4 and p8, Supplementary Table 2) was labelled by PCR using 30% dTTP substituted with DIG-dUTP. The hybridisation and DIG detection was carried out in accordance with manufacturer's instruction.

To create an ERD2B-2 knock-out plant (Figure 1; Supplementary Fig. S2; Supplementary Table 2), 5'- (956bp: primers p9 and p10) and 3'- (935bp: primers p11 and p12) targeting fragments were amplified from the genomic DNA located outside the ERD2B-2 coding region. These fragments were cloned either side of the 35S promoter driven *nptII* cassette in pMBL5DLΔS[50]. The transgene containing 817bp of 5' and 868bp of 3' targeting sequence were bulk-amplified by PCR (primers p13 and p14) and used to transform *P. patens*::*YFP-TM-ERD2B-1*. The stable transformants were identified by two rounds of G418 selection. The targeted single-copy knock-out plants were confirmed by PCR followed by Southern hybridisation using an *nptII*-specific probe (primers p20 and p21). For the removal of the selection cassette, protoplasts of the *YFP-TM-ERD2B-1*/*ERD2B-2KO* plant were transiently transformed with 10µg of the supercoiled rice actin promoter-driven Cre recombinase plasmid and allowed to grow on protoplast regeneration medium without selection. After 2 weeks, individual regenerants were sub-cultured onto fresh standard medium with and without selection. The marker removal was confirmed by PCR testing antibiotic-sensitive colonies for the absence of the selection cassette.

ERD2 plasmids from different eukaryotic organisms

Gene synthesis services by Eurofins Genomics were used to obtain desirable coding sequences (CDS) and designed to be delivered in pUC57 vectors with restriction sites flanking both ends (ClaI and BamHI). Specific ERD2 sequences were selected from an open source online database (NCBI).

For the bioassay analysis all CDS mentioned above were sub-cloned into an existing pJA31 vector, a double expression vector with a GUS internal marker previously described[23,52], via classical cloning utilising ClaI and BamHI restriction sites, substituting ERD2b gene and finally yielding TR2:GUS-

35s:oiERD2 (*O. lucimarinus*), TR2:GUS-35s:acERD2 (*A. castellanii*), TR2:GUS-35s:piERD2 (*P. infestans*), TR2:GUS-35s:ccERD2 (*C. crispus*), TR2:GUS-35s:gsERD2 (*G. sulphuraria*), TR2:GUS-35s:hsERD2 (*Homo sapiens*), TR2:GUS-35s:taERD2 (*Tardigrade sp.*), TR2:GUS-35s:tpERD2 (*T. pseudonana*), TR2:GUS-35s:pgERD2 (*P. graminis*), TR2:GUS-35s:klERD2 (*K. lactis*), TR2:GUS-35s:tbERD2 (*T. brucei*), TR2:GUS-35s:yERD2 (*S. cerevisiae*).

Human ERD2 derivatives

The construction of N-terminally tagged (YFP-TM-HsERD2) and C-terminally tagged (HsERD2-YFP) was carried out exactly as described previously for plant[23]. Primer BglII-hERD2 was used to introduce a BglII site and a short linker (Ile-Ser) to the HsERD2 N-terminus. Primer HsERD2-NheI was used to introduce an NheI site and a short linker (Ala-Ser-Ala) to the huERD2 C-terminus. Both constructs were built and inserted either into the double expression vector with a GUS internal marker (pRB17 and pRB19) or into a T-DNA vector for Agrobacterium-mediated plant cell transformation for expression under the transcriptional control of the TR2 promoter (pTRB21 and pTJCA107).

Mutagenesis of human ERD2 was carried out using standard primers for quick-change mutagenesis as described in supplementary table 2 and implemented on the untagged human ERD2 construct in the dual expression vector for quantitative Amy-HDEL cell retention assays, followed by subcloning into the T-DNA vector encoding YFP-TM-huERD2 to study the mutants via CLSM analysis.

Epitope tagged plant and human ERD2

All C-terminal tags were inserted by trailer PCR using long antisense primers (Supplementary table 2) annealing either with plant or human ERD2, followed by the trailer harbouring the relevant epitope coding region, a stop codon and restriction site XbaI, for PCR amplification in conjunction with cool35S (5'-CACTATCCTTCGCAAGACC-3') followed by ClaI-XbaI insertion into either the double expression vector with a GUS internal marker for cargo sorting assays (6 plasmids, see Supplementary table 1) or the T-DNA vector for CLSM analysis of the equivalent YFP-TM-ERD2 derivatives (6 further plasmids, see Supplementary table 1).

Deletions, hybrids and further derivatives of plant ERD2

To modify *Arabidopsis thaliana* ERD2b by deletions, chimeric hybrids and modified derivatives, a range of oligonucleotides were used either for direct trailer PCR or insertion of annealed primer pairs with sticky ends.

To replace the last 9 amino acids of ERD2 by the 9 amino acids of p24, the antisense primer ERD2b::p24tail was used combined with cool35S, followed by insertion into either the double expression vector with a GUS internal marker or the T-DNA vector for CLSM analysis. Mutagenesis of the di-lysine motif (KKSS) was done via Quick-change (Supplementary table 2), followed by the same subcloning reactions.

To test the influence of an alternative Golgi-retention signal (LPYS), the primers LPYSsense and LPYSanti were used to anneal a DNA fragment with NcoI and ClaI compatible sticky ends (encoding MSNS**LPYS**VKDVHYDNAKFRQR) to replace the YFP coding region in pFLA30[23] cut out by the same enzymes, resulting in the LPYS-TM-ERD2 coding region (pRB22). LPYS-TM-ERD2 and the control TM-ERD2 (pFLA33) were provided with a C-terminal YFP in the same way as described for ERD2 before[23], resulting in double expression vectors with a GUS internal marker plasmids pRB25 and pRB26, and the T-DNA vectors pTRB25 and pTRB26.

ERD2 constructs for re-distribution assays

To remove the di-leucine motif, the 5 last codons of ERD2b were removed by PCR amplification with primer ERD2bΔC5 anti, resulting in a coding region devoid of codons specifying the amino acids LQLPA, resulting in pTJCA88. The 35S-promoter driven ERD2b-YFP construct (pTJA10[23]) was re-constructed by replacing the 35S promoter by the weaker TR2 promoter by EcoRI-ClaI substitution, yielding pTMY1. To test the influence of over-expressed Amy and Amy-HDEL on several fluorescent ERD2 derivatives, the corresponding genes were recovered by HindIII digestions from pAmy and pAmy-HDEL respectively, followed by blunting with Klenow and further digestion with EcoRI. Plant expression vectors pTJCA88, pTFLA32, and pTMY1 were prepared by SnaBI-EcoRI digests followed by dephosphorylation, resulting in the dual expression plant vector plasmids pTRB6, pTRB7, pTRB8, pTRB9, pTMY3, pTMY4 (supplemental table 1).

Further fluorescent markers

The Golgi marker ST-RFP under the transcriptional control of the weak TR2 promoter in plasmid pTJA37 was described previously[23]. To generate an alternative Golgi-marker to specifically highlight *cis*-cisternae[30], the cytosolic N-terminus, the TM domain and a portion of the lumenal domain of MNS3 was amplified with MNS3 ClaI and MNS3 SalI from *N. benthamiana* protoplast cDNA, to replace the corresponding domains of ST-RFP[23], resulting in MNS3-RFP (pRB23). Subcloning into the T-DNA vector for Agrobacterium-mediated plant cell transformation for expression under the transcriptional control of the TR2 promoter resulted in pTRB23. ARF1-RFP was created by amplification of the ARF1 coding region as a NcoI-NheI fragment using primers ARF1-NcoI and ARF1-NheI and fused to an NheI-BamHI RFP fragment from pAW7 described earlier[11], to be expressed with the TR2 promoter.

Plant material and transient gene expression

Sterile grown *N. benthamiana*[52] plants, protoplast preparation, electroporation and subsequent incubation and harvesting were done as described previously[23]. The tobacco leaf infiltration procedure with soil grown plants was done as described too[53].

Confocal laser scanning microscopy

48 hours after infiltration, slides with tobacco leaf squares were prepared with tap water and imaged using an upright Zeiss LSM 880 Laser Scanning Microscope (Zeiss) with a PMT detector and a Plan-Apochromat 40x/1.4 oil DIC M27 objective using settings as described[23].

FRAP analysis

Samples to be used in fluorescence recovery after photobleaching (FRAP) studies were pre-treated to promote Golgi lock-down before analysis. 48 hours after infiltration, small sections of the infiltrated leaves were removed and kept in a solution containing latrunculin B solution to promote disruption of the cytoskeleton and stop Golgi movement. Infiltrated tobacco leaf squares (0.5 x 0.5 cm) were used for drug treatment preceding confocal imaging for photobleaching recovery studies, FRAP. To promote actin depolymerization and stop Golgi movement leaves were treated with latrunculin B[54]. Samples were submerged in 12µM solution of the latrunculin B (Cayman Chemical Co.) in water for one hour and analysed soon after.

Samples were then analysed via confocal laser scanning microscopy (CSLM). Golgi bodies showing both RFP and YFP fluorescence were selected as region of interest (ROI) and either bleached (black arrow-head) or kept as a control (white arrow-head).

Zen 2.3 black edition (Zeiss) software was used to record pre- and post-bleached signals and to modulate laser beam intensity. Signals were sampled before bleach treatment using standard confocal setting as described before. Bleaching was achieved by scanning with high-intensity illumination of selected regions of interest (ROI) and every 30 seconds after bleaching with low-intensity illumination following recommendation of previously published protocol[54].

Correlation analysis

Post-acquisition image processing was performed with the Zen 2.3 lite blue edition (Zeiss) and ImageJ ((http://rsb.info.gov/ij/)). Image analysis was undertaken using the ImageJ analysis program and the PSC co-localization plug-in[55] to calculate co-localization and to produce scatter plots as described before[11].

Enzyme assays

Measurement of α-amylase activity and calculation of the secretion index (ratio of extracellular to intracellular enzyme activities) were done as described previously[23,51,56]. For GUS-normalised effector dose-response assays, the GUS enzyme essay was used. To reach best transfection practice (BTP), new dual expression plasmid preparations were first subject to transfection quality control by measuring the GUS activity after standard electroporations as described earlier[23]. However, plasmid dilutions were used to determine the point at which GUS activity starts to reach a plateau. A relative activity of 30 units (given in ΔOD per mL protoplast suspension and per hour enzyme incubation) prior to plateau conditions was deemed acceptable for BTP. Plasmids that reached the GUS activity plateau with lower than 30 units were deemed unsuitable and were discarded. For GUS-normalised comparisons of different effector plasmids and for dose-response assays, plasmid doses were strictly determined volumetrically as a percentage of the maximum dose resulting in 30 GUS units.

Generation of transgenic plants by leaf-disk transformation

N. benthamiana plants were obtained via Agrobacterium infection of leaf disks[57]. Selection of transformants was accomplished in MS medium supplemented with 3% sucrose and containing 100 µg/mL kanamycin and 250 µg/mL cefotaxime. Regenerated plants were analysed and scored by CLSM.

In vivo labelling and immuno-precipitation

In vivo labelling of *N. benthamiana* protoplast suspensions was essentially done as described previously[58] with the following modifications: 4 repeats of standard electroporations[23] yielding 2.5ml protoplast suspensions each were pooled together for each sample (mock, Amy-HDEL and Amy-HDEL + ERD2-HA). After 1hour rest in a standard 9cm Petri Dish, the 10 mL pools were centrifuged at 100 rpm in conical tubes, followed by the removal of the dead cell pellet and the majority of the medium underneath the floating band of live cells. Protoplasts were then resuspended in a final volume of 2 mL TEX buffer and supplemented with 0.5 mL TEX containing 500 mCi/mL Pro-mix (70% 35S-methionine and 30% 35S-cysteine, Amersham Life Science), followed by incubation for 8 hours at room temperature in the dark and harvesting of washed cell pellets and clear culture medium using the standard procedure. Culture

medium was kept on ice for further work. Lysis of washed cell pellets was carried out by resuspending the washed cell pellet with 950 microlitres of ice-cold homogenization buffer (200 mM Tris-Cl, pH 8.0, 300 mM NaCl, 1% Triton X-100, 1 mM EDTA, and 2 mM phenylmethylsulfonyl fluoride). The homogenate was then centrifuged for 5 min in a minicentrifuge, and the supernatant was kept on ice for further work.

Immunoprecipitations were either carried out with 500 microlitres of culture medium or 200 microlitres of the cell lysis fraction, each representing 20% of the total labelled protoplast suspension, allowing direct calculation of secretion indices after quantification of signals from medium and cells. All manipulations were performed on ice or at 4°C using ice-cold buffers. NET gel buffer (50 mM Tris-Cl, pH 7.5, 150 mM NaCl, 1 mM EDTA, 0.1% Nonidet P-40, and 0.02% NaN3 and supplemented with 0.25% gelatin) was used to bring either the medium or the cell lysis fraction up to 1mL. After centrifugation to remove any remaining debris, the supernatant was incubated on ice with an excess of either anti-HA antibody or anti-amylase antibodies for 1 hour, allowing for the complete precipitation of all ERD2 or Amy-HDEL proteins after addition of protein A-sepharose and subsequent washing steps as described[58]. After the last wash, all liquid was removed from the washed protein A-sepharose pellets using a refined glass capillary. The pellets were then supplemented with thirty microlitres of SDS-PAGE loading buffer (200 mM Tris-Cl, pH 8.8, 5 mM EDTA, 1 M sucrose, 20 mM DTT, 2.5% SDS, 0.1% bromophenol blue) and the suspensions were incubated at 90°C for 5min. The sample was then centrifuged for 2 min in a minicentrifuge and 20 microlitres was separated on SDS-PAGE (10% strength), followed by electroblotting on nitrocellulose. Dried nitrocellulose sheets were analysed by phosphorimaging. Sample peak selection and detection were achieved by Aida version 4.14 and detector Fuji FLA-5000 respectively. Error bars are standard errors of three independent repeats. Arbitrary units of pixel intensity are compared relative to other values within the same experiment, and corrected for the 2/3 ratio of amino acids methionine and cysteine in ERD2 relative to Amylase.

Declarations

Acknowledgments

The work in this article was in part supported by the European Union (projects HPRN-CT-2002-00262 and LSH-2002-1.2.5 – 2), the Biotechnology and Biological Sciences Research Council (BBSRC) project nr. BB/D016223/1 and The Leverhulme Trust (F/10 105/E). Jonas C. Alvim is grateful for a PhD scholarship awarded from the Conselho Nacional de Desenvolvimento Científico e Tecnológico – Brasil (CNPq 201192/2014-4). Robert M. Bolt is grateful for a Faculty of Biological Sciences PhD studentship funded by the University of Leeds. Reese's Cups (Hershey Company, 1025 Reese Ave, Hershey, PA 17033) is thanked for providing food for thought. Jack Ranger and Nicoletta Bencka are thanked for contributing to the construction of recombinant plasmids (Supplementary table 1). David Gershlick is thanked for scientific discussion and critically reading the manuscript.

References

1) TANGEMO, C., RONCHI, P., COLOMBELLI, J., HASELMANN, U., SIMPSON, J. C., ANTONY, C., STELZER, E. H. K., PEPPERKOK, R. & REYNAUD, E. G. 2011. A novel laser nanosurgery approach supports de novo Golgi biogenesis in mammalian cells. Journal of Cell Science, 124, 978-987.

2) GLICK, B. S. & LUINI, A. 2011. Models for Golgi traffic: a critical assessment. Cold Spring Harb Perspect Biol, 3, a005215.

3) LUJAN, P. & CAMPELO, F. 2021. Should I stay or should I go? Golgi membrane spatial organization for protein sorting and retention. Archives of Biochemistry and Biophysics, 707, 108921.

4) GOLDSTEIN, J. L., ANDERSON, R. G. W. & BROWN, M. S. 1979. COATED PITS, COATED VESICLES, AND RECEPTOR-MEDIATED ENDOCYTOSIS. Nature, 279, 679-685.

5) VONFIGURA, K. & HASILIK, A. 1986. LYSOSOMAL-ENZYMES AND THEIR RECEPTORS. Annual Review of Biochemistry, 55, 167-193.

6) DUNCAN, J. R. & KORNFELD, S. 1988. Intracellular movement of two mannose 6-phosphate receptors: return to the Golgi apparatus. J Cell Biol, 106, 617-28.

7) SEAMAN, M. N. J. 2005. Recycle your receptors with retromer. Trends in Cell Biology, 15, 68-75.

8) SEAMAN, M. N. J., MARCUSSON, E. G., CEREGHINO, J. L. & EMR, S. D. 1997. Endosome to Golgi retrieval of the vacuolar protein sorting receptor, Vps10p, requires the function of the VPS29, VPS30, and VPS35 gene products. Journal of Cell Biology, 137, 79-92.

9) DASILVA, L. L., TAYLOR, J. P., HADLINGTON, J. L., HANTON, S. L., SNOWDEN, C. J., FOX, S. J., FORESTI, O., BRANDIZZI, F. & DENECKE, J. 2005. Receptor salvage from the prevacuolar compartment is essential for efficient vacuolar protein targeting. Plant Cell, 17, 132-48.

10) DASILVA, L. L., FORESTI, O. & DENECKE, J. 2006. Targeting of the plant vacuolar sorting receptor BP80 is dependent on multiple sorting signals in the cytosolic tail. Plant Cell, 18, 1477-97.

11) FORESTI, O., GERSHLICK, D. C., BOTTANELLI, F., HUMMEL, E., HAWES, C. & DENECKE, J. 2010. A Recycling-Defective Vacuolar Sorting Receptor Reveals an Intermediate Compartment Situated between Prevacuoles and Vacuoles in Tobacco. Plant Cell, 22, 3992-4008.

12) PELHAM, H. R. 1988. Evidence that luminal ER proteins are sorted from secreted proteins in a post-ER compartment. Embo j, 7, 913-8.

13) DEAN, N. & PELHAM, H. R. B. 1990. RECYCLING OF PROTEINS FROM THE GOLGI COMPARTMENT TO THE ER IN YEAST. Journal of Cell Biology, 111, 369-377.

14) SEMENZA, J. C., HARDWICK, K. G., DEAN, N. & PELHAM, H. R. B. 1990. ERD2, A YEAST GENE REQUIRED FOR THE RECEPTOR-MEDIATED RETRIEVAL OF LUMINAL ER PROTEINS FROM THE

SECRETORY PATHWAY. Cell, 61, 1349-1357.

15) LEWIS, M. J. & PELHAM, H. R. 1990. A human homologue of the yeast HDEL receptor. Nature, 348, 162-3.

16) LEWIS, M. J. & PELHAM, H. R. 1992a. Ligand-induced redistribution of a human KDEL receptor from the Golgi complex to the endoplasmic reticulum. Cell, 68, 353-64.

17) Tang, B.L., Wong, S.H., Qi, X.L., Low, S.H., and Hong, W. (1993). Molecular cloning, characterization, subcellular localization and dynamics of p23, the mammalian KDEL receptor. J. Cell Biol. 120: 325–338.

18) Li, J., Zhao-Hui, C., Batoux, M., Nekrasov, V., Roux, M., Chinchilla, D., Zipfel, C., and Jones, J.D.G. (2009). Specific ER quality control components required for biogenesis of the plant innate immune receptor EFR. Proc. Natl. Acad. Sci. USA 106: 15973–15978.

19) BOEVINK, P., OPARKA, K., CRUZ, S. S., MARTIN, B., BETTERIDGE, A. & HAWES, C. 1998. Stacks on tracks: the plant Golgi apparatus traffics on an actin/ER network. Plant Journal, 15, 441-447.

20) MAJOUL, I., STRAUB, M., HELL, S. W., DUDEN, R. & SOLING, H. D. 2001. KDEL-cargo regulates interactions between proteins involved in COPI vesicle traffic: Measurements in living cells using FRET. Developmental Cell, 1, 139-153.

21) CABRERA, M., MUÑIZ, M., HIDALGO, J., VEGA, L., MARTÍN, M. E. & VELASCO, A. 2003. The Retrieval Function of the KDEL Receptor Requires PKA Phosphorylation of Its C-Terminus. Molecular Biology of the Cell, 14, 4114-4125.

22) BRÄUER, P., PARKER, J. L., GERONDOPOULOS, A., ZIMMERMANN, I., SEEGER, M. A., BARR, F. A. & NEWSTEAD, S. 2019. Structural basis for pH-dependent retrieval of ER proteins from the Golgi by the KDEL receptor. Science 363, 1103-1107.

23) SILVA-ALVIM, F. A. L., AN, J., ALVIM, J. C., FORESTI, O., GRIPPA, A., PELGROM, A. J. E., ADAMS, T. L., HAWES, C. & DENECKE, J. 2018. Predominant Golgi-residency of the plant K/HDEL receptor is essential for its function in mediating ER retention. Plant Cell, 30, 2174-2196.

24) TOWNSLEY, F. M., FRIGERIO, G. & PELHAM, H. R. B. 1994. RETRIEVAL OF HDEL PROTEINS IS REQUIRED FOR GROWTH OF YEAST-CELLS. Journal of Cell Biology, 127, 21-28.

25) MONTESINOS, J. C., PASTOR-CANTIZANO, N., ROBINSON, D. G., MARCOTE, M. J. & ANIENTO, F. 2014. Arabidopsis p24 delta 5 and p24 delta 9 facilitate Coat Protein I-dependent transport of the K/HDEL receptor ERD2 from the Golgi to the endoplasmic reticulum. Plant Journal, 80, 1014-1030.

26) HSU, V. W., SHAH, N. & KLAUSNER, R. D. 1992. A brefeldin A-like phenotype is induced by the overexpression of a human ERD-2-like protein, ELP-1. Cell, 69, 625-35.

27) AOE, T., CUKIERMAN, E., LEE, A., CASSEL, D., PETERS, P. J. & HSU, V. W. 1997. The KDEL receptor, ERD2, regulates intracellular traffic by recruiting a GTPase-activating protein for ARF1. Embo Journal, 16, 7305-7316.

28) CONTRERAS, I., ORTIZ-ZAPATER, E. & ANIENTO, F. 2004a. Sorting signals in the cytosolic tail of membrane proteins involved in the interaction with plant ARF1 and coatomer. Plant Journal, 38, 685-698.

29) CONTRERAS, I., YANG, Y., ROBINSON, D. G. & ANIENTO, F. 2004b. Sorting signals in the cytosolic tail of plant p24 proteins involved in the interaction with the COPII coat. Plant Cell Physiol, 45, 1779-86.

30) SCHOBERER, J., KONIG, J., VEIT, C., VAVRA, U., LIEBMINGER, E., BOTCHWAY, S. W., ALTMANN, F., KRIECHBAUMER, V., HAWES, C. & STRASSER, R. 2019. A signal motif retains Arabidopsis ER-alpha-mannosidase I in the cis-Golgi and prevents enhanced glycoprotein ERAD. Nat Commun, 10, 3701.

31) GRANT, B. D. & DONALDSON, J. G. 2009. Pathways and mechanisms of endocytic recycling. Nat Rev Mol Cell Biol, 10, 597-608.

32) MACER, D. R. & KOCH, G. L. 1988. Identification of a set of calcium-binding proteins in reticuloplasm, the luminal content of the endoplasmic reticulum. Journal of Cell Science, 91, 61-70.

33) JACKSON, M. R., NILSSON, T. & PETERSON, P. A. 1990. Identification of a consensus motif for retention of transmembrane proteins in the endoplasmic reticulum. The EMBO journal, 9, 3153-3162.

34) PFEFFER, S. R. 2007. Unsolved mysteries in membrane traffic. Annu Rev Biochem, 76, 629-45.

35) Phillipson, B.A., Pimpl, P., Lamberti Pinto daSilva, P., Crofts, A.J., Taylor, J.P., Movafeghi, A., Robinson, D.G., and Denecke, J. (2001). Secretory Bulk Flow of Soluble Proteins Is Efficient and COPII Dependent. Plant Cell 13, 2005-2020.

36) COSSON, P. & LETOURNEUR, F. 1994. Coatomer interaction with di-lysine endoplasmic reticulum retention motifs. Science, 263, 1629-31.

37) LETOURNEUR, F., GAYNOR, E. C., HENNECKE, S., DEMOLLIERE, C., DUDEN, R., EMR, S. D., RIEZMAN, H. & COSSON, P. 1994. COATOMER IS ESSENTIAL FOR RETRIEVAL OF DILYSINE-TAGGED PROTEINS TO THE ENDOPLASMIC-RETICULUM. Cell, 79, 1199-1207.

38) PELHAM, H. R. B. 1994. ABOUT TURN FOR THE COPS. Cell, 79, 1125-1127.

39) Ito, Y., Uemura, T. & Nakano, A. 2018. The Golgi entry core compartment functions as a COPII independent scaffold for ER-to-Golgi transport in plant cells Journal of Cell Science 131, jcs203893. doi:10.1242/jcs.203893

40) APPENZELLER-HERZOG, C. & HAURI, H. P. 2006. The ER-Golgi intermediate compartment (ERGIC): in search of its identity and function. Journal of Cell Science, 119, 2173-2183.

41) SAITO, K., CHEN, M., BARD, F., CHEN, S., ZHOU, H., WOODLEY, D., POLISCHUK, R., SCHEKMAN, R. & MALHOTRA, V. 2009. TANGO1 facilitates cargo loading at endoplasmic reticulum exit sites. Cell, 136, 891-902.

42) SAITO, K., YAMASHIRO, K., ICHIKAWA, Y., ERLMANN, P., KONTANI, K., MALHOTRA, V. & KATADA, T. 2011. cTAGE5 mediates collagen secretion through interaction with TANGO1 at endoplasmic reticulum exit sites. Mol Biol Cell, 22, 2301-8.

43) RAOTE, I., ORTEGA-BELLIDO, M., SANTOS, A. J. M., FORESTI, O., ZHANG, C., GARCIA-PARAJO, M. F., CAMPELO, F. & MALHOTRA, V. 2018. TANGO1 builds a machine for collagen export by recruiting and spatially organizing COPII, tethers and membranes. eLife, 7:e32723.

44) SATO, K., SATO, M. & NAKANO, A. 2001. Rer1p, a retrieval receptor for endoplasmic reticulum membrane proteins, is dynamically localized to the Golgi apparatus by coatomer. J Cell Biol, 152, 935-44.

45) WANG, J., YAN, C., LI, Y., HIRATA, K., YAMAMOTO, M., YAN, N. & HU, Q. 2014. Crystal structure of a bacterial homologue of SWEET transporters. Cell Research, 24, 1486-1489.

46) XU, Y., TAO, Y., CHEUNG, L. S., FAN, C., CHEN, L.-Q., XU, S., PERRY, K., FROMMER, W. B. & FENG, L. 2014. Structures of bacterial homologues of SWEET transporters in two distinct conformations. Nature, 515, 448-452.

47) LEE, Y., NISHIZAWA, T., YAMASHITA, K., ISHITANI, R. & NUREKI, O. 2015. Structural basis for the facilitative diffusion mechanism by SemiSWEET transporter. Nature Communications, 6, 6112.

Methods References

48) CASADABAN, M. J. & COHEN, S. N. 1980. Analysis of gene control signals by DNA fusion and cloning in Escherichia coli. J Mol Biol, 138, 179-207.

49) KNIGHT, C.D., COVE, D.J., CUMING, A.C., QUATRANO, R.S. (2002) Moss gene technology. In: Molecular Plant Biology Vol. 2: pp. 285-299. Gilmartin PM, Bowler C (Eds) Oxford University Press.

50) CAINE, R. S., CHATER, C. C., KAMISUGI, Y., CUMING, A. C., BEERLING, D. J., GRAY, J. E. & FLEMING, A. J. 2016. An ancestral stomatal patterning module revealed in the non-vascular land plant Physcomitrella patens. Development, 143, 3306-3314.

51) GERSHLICK, D. C., LOUSA CDE, M., FORESTI, O., LEE, A. J., PEREIRA, E. A., DASILVA, L. L., BOTTANELLI, F. & DENECKE, J. 2014. Golgi-dependent transport of vacuolar sorting receptors is regulated by COPII, AP1, and AP4 protein complexes in tobacco. Plant Cell, 26, 1308-29.

52) GOODIN, M. M., ZAITLIN, D., NAIDU, R. A. & LOMMEL, S. A. 2008. Nicotiana benthamiana: its history and future as a model for plant-pathogen interactions. Mol Plant Microbe Interact, 21, 1015-26.

53) SPARKES, I.A., RUNIONS, J., KEARNS, A., AND HAWES, C. (2006). Rapid, transient expression of fluorescent fusion proteins in tobacco plants and generation of stably transformed plants. Nat. Protoc. 1: 2019–2025.

54) BRANDIZZI, F., SNAPP, E. L., ROBERTS, A. G., LIPPINCOTT-SCHWARTZ, J. & HAWES, C. 2002. Membrane protein transport between the endoplasmic reticulum and the Golgi in tobacco leaves is energy dependent but cytoskeleton independent: evidence from selective photobleaching. Plant Cell, 14, 1293-309.

55) FRENCH, A. P., MILLS, S., SWARUP, R., BENNETT, M. J. & PRIDMORE, T. P. 2008. Colocalization of fluorescent markers in confocal microscope images of plant cells. Nat Protoc, 3, 619-28.

56) FORESTI, O., DASILVA, L. L. & DENECKE, J. 2006. Overexpression of the Arabidopsis syntaxin PEP12/SYP21 inhibits transport from the prevacuolar compartment to the lytic vacuole in vivo. Plant Cell, 18, 2275-93.

57) DENECKE, J., BOTTERMAN, J. & DEBLAERE, R. 1990. Protein secretion in plant cells can occur via a default pathway. Plant Cell, 2, 51-9.

58) CROFTS, A. J., LEBORGNE-CASTEL, N., PESCA, M., VITALE, A. & DENECKE, J. 1998. BiP and calreticulin form an abundant complex that is independent of endoplasmic reticulum stress. Plant Cell, 10, 813-24.

Figures

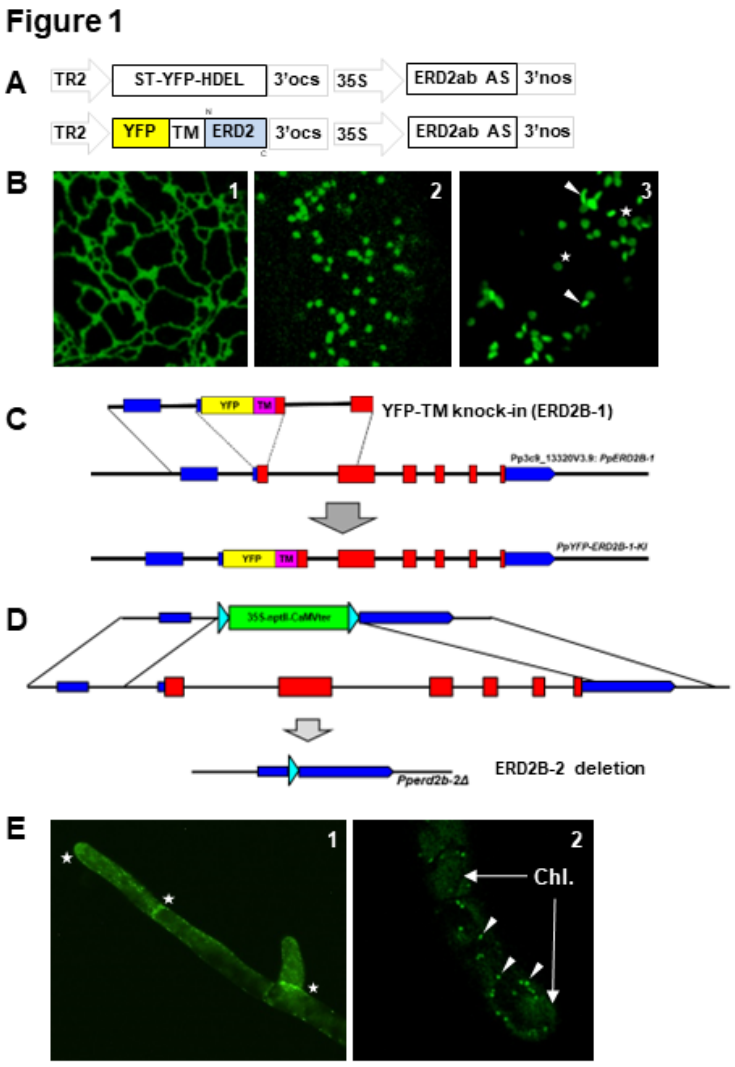

Figure 1

Genetic validation of YFP-TM-ERD2 by stable transformation in *Nicotiana benthamiana* and *Physcomitrium patens*

(A) Schematic of *N. benthamiana* ERD2ab antisense (AS) construct driven by the strong constitutive CaMV35S promoter (35S), combined with fluorescent markers expressed under the weak TR2 promoter

on the same T-DNA.

(B) Confocal laser scanning microscopy of stably transformed *N. benthamiana* in leaf epidermis cells of regenerating shoots in vitro (B1, B2) and root cortex cells of seedlings from the next generation of YFP-TM-ERD2 plants (B3). Notice that ST-YFP-HDEL labels the ER whilst YFP-TM-ERD2 only labels Golgi bodies. In roots, Golgi-stacks are either viewed from the side (white arrow heads) or from top/bottom (white stars), giving rise to the typical doughnut shapes.

(C) Schematic of YFP-TM targeted gene knock-in onto *Pp*ERD2B-1 (Pp3c9_13230V3.9), in which the YFP-TM coding portion (Silva-Alvim et al., 2018) was recombined into the first protein-coding exon by marker-free transformation, leading to expression of a YFP-TM-ERD2 derivative under the transcriptional control of the native promoter in *P. patens*.

(D) Schematic of *Pp*ERDB2-2 (Pp3c15_12830) knockout by complete deletion of the second ERD2 gene by targeted replacement with a selection cassette flanked with loxP sites enabling the subsequent deletion of the marker by transient expression of Cre recombinase. Lines positively tested for both knock-in and knock-out events (Supplementary figures 1, 2) showed normal growth.

(E) YFP-TM-PpERD2 expression under its native promoter in *P. patens*. E1) Notice stronger expression near growing tips and newly formed cell plates. E2) At high magnification, distinguish punctate structures from weak autofluorescence of chloroplasts (Chl.).

Figure 2

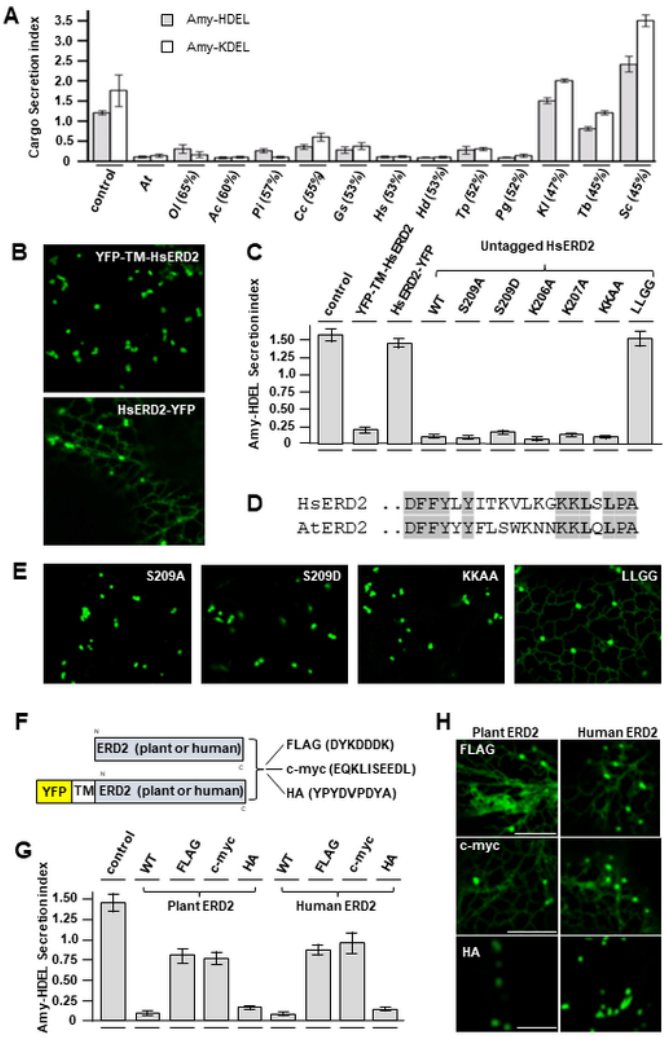

Figure 2

ERD2 Function and Golgi Residency is Conserved Amongst Eukaryotes

(A) Retention assay using protoplasts showing the secretion index (ratio extra/intracellular Amy-HDEL activity) with cargo alone or with co-expressed *A. thaliana* ERD2b (At) and 12 further ERD2 orthologs from the eukaryotes *Ostreococcus lucimarinus* (Oi), *Acanthamoeba castellanii* (Ac), *Phytophthora*

infestans (Pi), *Chondrus crispus* (Cc), *Galdieria sulphuraria* (Gs), *Homo sapiens* (HsERD2), *Hypsibius dujardini* (Hd), *Thalassiosira pseudonana* (Tp), *Puccinia graminis* (Pg), *Kluyveromyces lactis* (KlERD2), *Trypanosoma brucei* (Tb) and *Saccharomyces cerevisiae* (Sc). Transfection efficiencies were normalised by the internal marker GUS established at 5 standard OD units as described in materials and methods. Percentages in brackets refer to the sequence identity with AtERD2b.

Notice that cargo retention function is abolished when less than 50% sequence identity remains.

(B) CLSM analysis of two human ERD2 fusions (YFP-TM-HsERD2 and HsERD2-YFP constructed as described before[23]. Notice that only the C-terminal YFP fusion causes partial ER localisation.

(C) Retention assays as in A) but either comparing the two HsERD2 fluorescent variants from B) or a comparison of untagged hsERD2 (WT) with point –mutations in the HsERD2 C-terminus indicated above each lane. KKAA refers to the double mutant combining K206A and K207A. LLGG refers to the double mutant combining L208G and L210G. Notice that the C-terminal YFP fusion has lost biological activity. Notice also that only the LLGG mutant has lost biological activity when untagged HsERD2 is analysed. A full dose response for the KKAA double mutant is provided in Supp. Figure 3.

(D) C-terminal amino acid sequences of human (KDELR2) and *A. thaliana* ERD2B. Conserved residues are highlighted grey and the conserved di-leucine motif is highlighted bold.

(E) CLSM analysis of selected mutants from C) but in the YFP-TM-HsERD2 configuration. Silent mutations in panel C) retain the Golgi localisation, whilst the inactive LLGG mutant displays partial ER localisation.

(F) Schematic of C-terminal fusions to plant and human ERD2 for functional assays (upper) and the fluorescent derivative for CLSM analysis (lower schematic).

(G) Secretion index of Amy-HDEL, co-expressed with either wild type human or plant ERD2 compared to the three different C-terminal modifications in each case. Constant levels of ERD2 encoding plasmids were co-transfected (yielding 5 standard OD units). In both instances, the addition of a FLAG or c-myc tag strongly reduced function, whilst most of the activity was maintained for each ortholog after adding the HA tag.

(H) Localisation of human and plant ERD2 fluorescent fusions with C-terminal FLAG, c-myc and HA tags. Notice that FLAG and c-myc additions cause an ER-Golgi localisation, whilst the addition of an HA tag does not affect the Golgi localisation of YFP-TM-ERD2 for both orthologs.

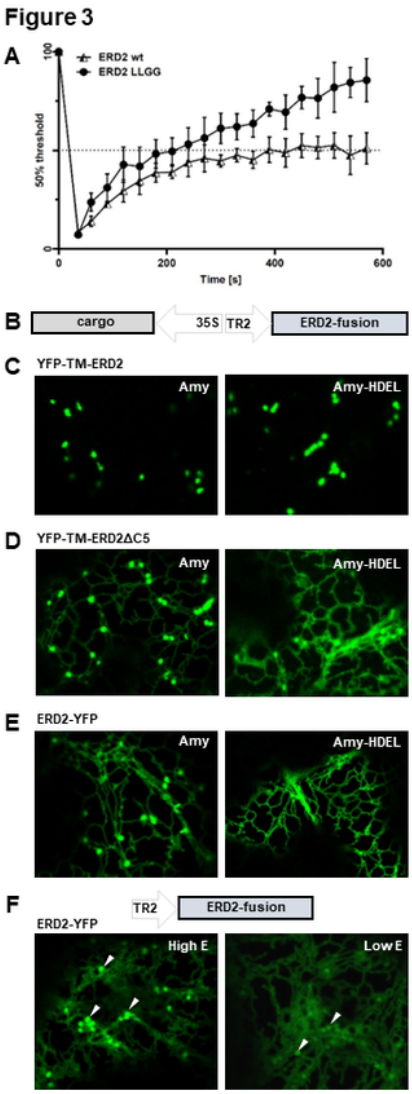

Figure 3

FRAP and redistribution assays identify a Golgi-retention signal at the ERD2 C-terminus

(A) Fluorescence recovery after photobleaching comparing wild type ERD2 and the LLGG mutant. ERD2 recovery to 50% (400 seconds) took almost twice the time of the LLGG mutant (240 seconds). LLGG mutant recovery reached 85%, whereas wild type ERD2 remained at around 50%.

(B) Schematic of dual expression T-DNA constructs used to co-express fluorescent ERD2 fusions with cargo (either secreted Amy or the ERD2-ligand AmyHDEL).

(C) Golgi localisation of YFP-TM-ERD2 co-expressed with Amy and Amy-HDEL. Distribution remains unchanged for both cargo.

(D) Dual ER-Golgi localisation of YFP-TM-ERD2ΔC5 co-expressed with Amy and a more prominent ER localisation when co-expressed with Amy-HDEL.

(E) Dual ER-Golgi localisation of ERD2-YFP co-expressed with Amy. The re-distribution of ERD2-YFP to the ER by co-expressed Amy-HDEL is even more drastic compared to that of the deletion mutant in panel D).

(F) Schematic of the T-DNA for expression analysis of the ERD2-fusion alone. Golgi bodies (arrows) are labelled by ERD2-YFP more visibly during high cellular expression, whereas punctae are much fainter relative to the ER fluorescence at low expression (imaged at higher detector gain).

Figure 4

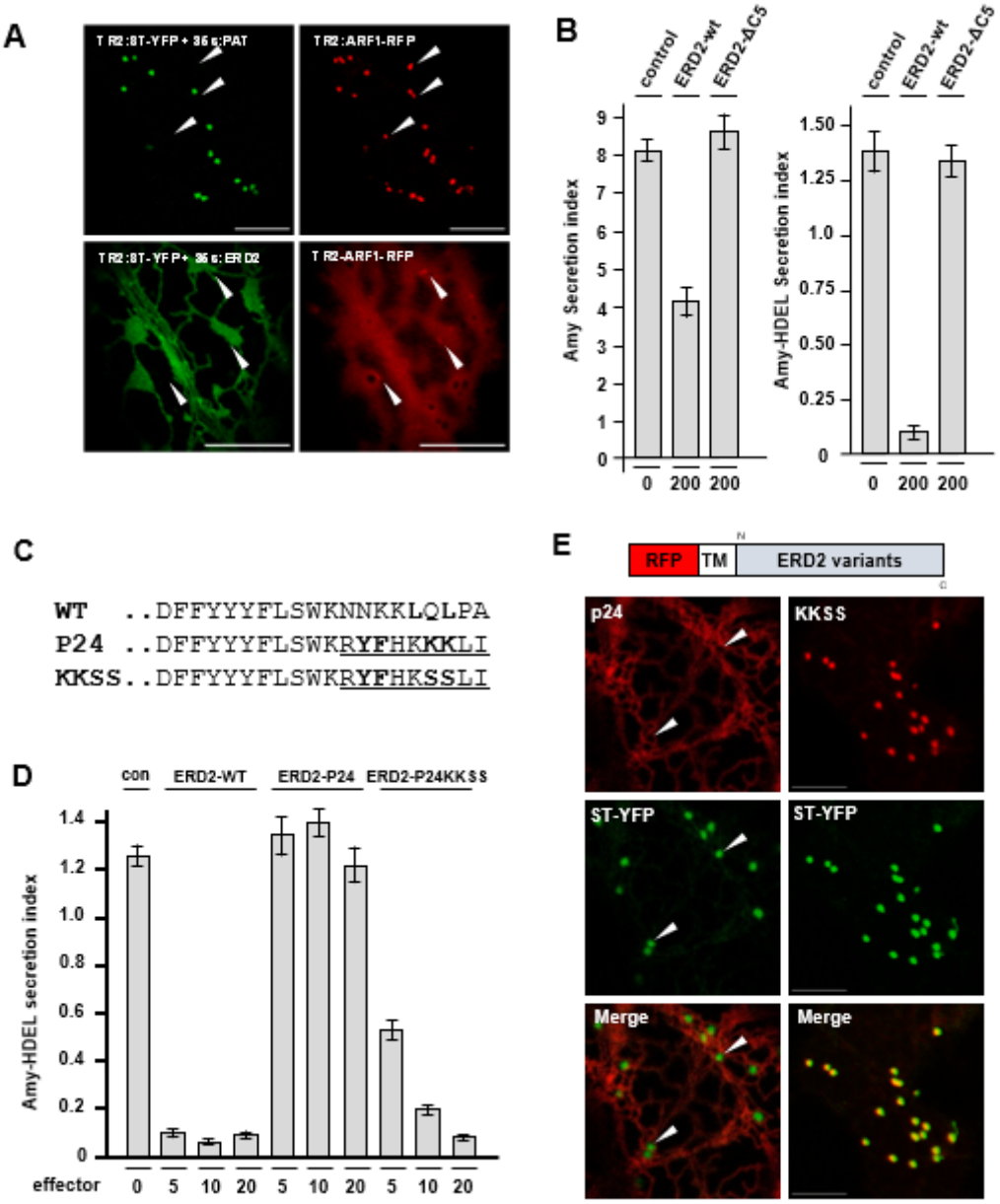

Figure 4

ERD2 activity is incompatible with COPI-mediated transport.

(A) ARF1-RFP localisation in relation to co-expressed Golgi marker ST-YFP together with either co-expressed cytosolic mock protein (PAT, upper panel) as control, or ERD2 (lower panel). Notice that under control conditions the subcellular localisation of ARF1-RFP is mainly in punctate structures, colocalising with the Golgi marker and additional extra-Golgi structures (white arrow heads). Upon co-expression of ERD2, the Golgi-marker redistributes to the ER network, whilst ARF1-RFP is mainly cytosolic. White arrow heads point at post-Golgi structures that remain.

(B) Effect of saturating ERD2 overexpression (given in standard GUS OD units below each lane) on secretion of either Amy or Amy-HDEL. Notice that inhibition of constitutive secretion is not observed for the deletion mutant ERD2-ΔC5).

(C) C-terminal amino acid sequences of ERD2 wild type (WT) and two variants in which the last 9 amino acids of ERD2 is replaced by the corresponding region of P24 (underlined.) The proposed COPII ER export signal of p24[29] is in bold, as is the dileucine motif in the WT sequence, the relevant lysines of the canonical COPI transport motif in the p24 variant and finally the mutant serines in the KKSS variant.

(D) Dose-response assay measuring the influence of co-transfected C-terminal ERD2 variants (given in standard GUS OD units below each lane) on AmyHDEL secretion. ERD2WT mediates strong cell retention whilst the P24 fusion shows no retention activity. The KKSS mutant of the p24 fusion restores the retention activity at the highest dose.

(E) Localisation of p24 and KKSS hybrids incorporated into fluorescent ERD2 fusion proteins. The p24 C-terminus mediates complete ER localisation of the resulting ERD2 fusion whilst the KKSS mutant shows high steady state levels at the Golgi.

Figure 5

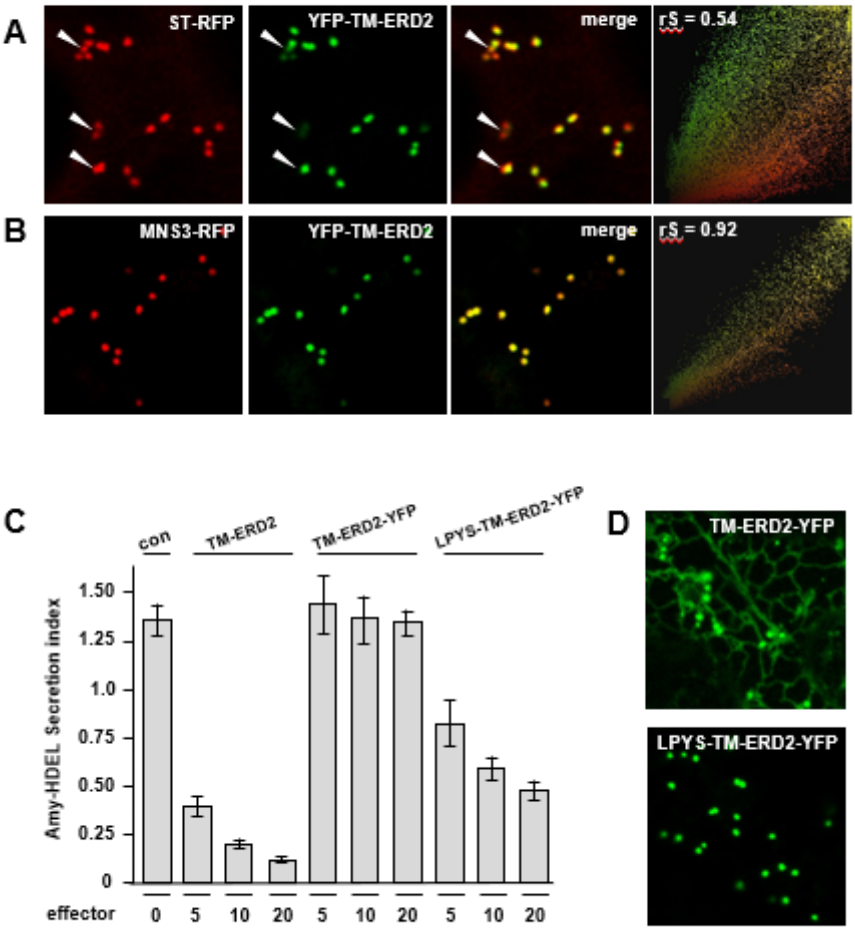

Figure 5

Reactivation of ERD2-YFP with a novel cis-Golgi retention motif

(A) Comparative Golgi distribution between ST-RFP and YFP-TM-ERD2. Although both labelling punctae, an rS value of 0.54 highlights a cis-trans Golgi segregation of YFP-TM-ERD2 and ST-RFP, respectively. This is also visible in regions identified with white arrow heads.

(B) When compared with MNS3-RFP instead, the shared cis-Golgi localisation of YFP-TM-ERD2 is clearly demonstrated by an rS value of 0.92.

(C) Retention of AmyHDEL by ERD2 fusion variants at increasing concentrations. As previously published, TM-ERD2 effectively retains AmyHDEL at low and high concentrations. Meanwhile the C-terminal addition of YFP completely abolishes retention, regardless of increasing concentration. However, the N-terminal addition of the LPYS Golgi retention motif does allow significant activity to return with increasing concentration.

(D) N-terminal addition of LPYS causes redistribution of TM-ERD2-YFP exclusively to the Golgi, in agreement with reactivation in secretion assays.

Figure 6

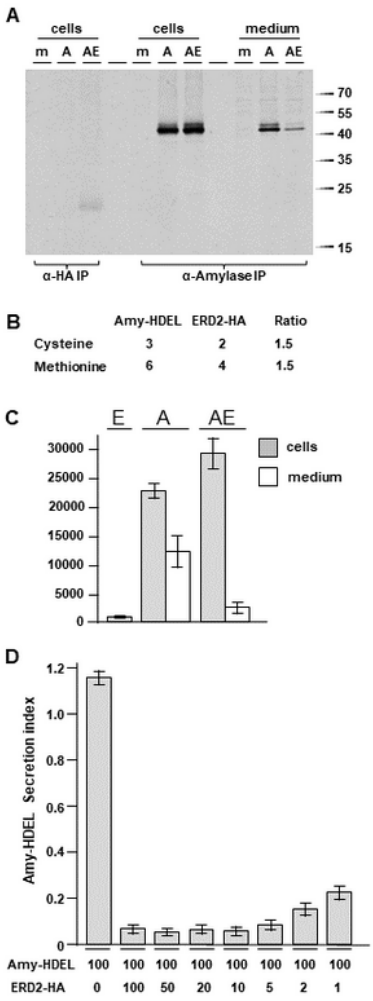

Figure 6

Receptor-recycling cannot explain the observed receptor-ligand stoichiometry

Transient expression in which both receptor and ligand were expressed from dual expression vectors harbouring GUS as reference marker for transfection efficiency and expressed at identical GUS units.

(A) Immunoprecipitated ERD2-HA and co-expressed Amy-HDEL separated by SDS-page, followed by blotting on nitrocellulose and visualisation via phosphorimaging. Molecular weight markers are given on the right in kilo-daltons.

(B) Table showing the total number of cysteine and methionine residues in cargo and receptor. Relative radioactivity units measured for ERD2-HA by phosphorimaging must be multiplied by 1.5 to permit comparison with units from Amy-HDEL to permit calculation of relative number of molecules.

(C) Phosphorimaging quantification (arbitrary relative units) of signals from 3 different nitrocellulose blots as in A) showing the radioactivity from transiently expressed ERD2-HA and co-expressed Amy-HDEL (A) from cells and medium. Notice that Amy-HDEL radioactivity is extremely high compared to that of ERD2-HA (955 units), increasing from 22838 to 29284 units in the cells due to co-expressed ERD2-HA. Correcting for the number of cysteine and methionine residues, the introduced ERD2-HA is the equivalent of 1433 units, approximately 4.5 – fold lower than the increase in cellular Amy-HDEL molecules (6446 units).

(D) Retention of AmyHDEL where the maximum receptor levels from panel A are co-transfected (second lane), followed by consecutive dilution of the receptor plasmid up to 100 fold (last lane). Notice that a strong reduction in Amy-HDEL secretion compared to the control (first lane) is still observed even after 100-fold dilution of the receptor plasmid (last lane).

Supplementary Files

This is a list of supplementary files associated with this preprint. Click to download.

- Supplementarytable1plasmidsusedinthisstudy.docx
- Supplementarytable2primerlist.docx
- Supplementaryfigurelegends.docx
- Supplementalfigures.pptx